



# Quantitative proteomic analysis of urinary exosomes in kidney stone patients

Qing Wang, Yi Sun, Yuanyuan Yang, Cong Li, Jiaqiao Zhang, Shaogang Wang

Department of Urology, Tongji Hospital, Tongji Medical College, Huazhong University of Science and Technology, Wuhan, China

**Contributions:** (I) Conception and design: Q Wang, S Wang; (II) Administrative support: S Wang; (III) Provision of study materials or patients: C Li, S Wang; (IV) Collection and assembly of data: Q Wang, Y Sun, J Zhang, S Wang; (V) Data analysis and interpretation: Q Wang, Y Sun, Y Yang; (VI) Manuscript writing: All authors; (VII) Final approval of manuscript: All authors.

**Correspondence to:** Shaogang Wang. Department of Urology, Tongji Hospital, Tongji Medical College, Huazhong University of Science and Technology, Wuhan 430030, China. Email: sgwangtjm@163.com.

**Background:** Increased urinary exosomes are associated with kidney stones but how they work is unknown. In this study, we aim to identify dysregulated proteins in urinary exosomes from kidney stone patients and to explore the potential role of exosomal proteins in nephrolithiasis.

**Methods:** First morning voids were collected from participants. Urinary exosomes were isolated via ultracentrifugation. Label free liquid chromatography-tandem mass spectrometry was performed to analyze the proteome of urine exosomes from three kidney stone patients and three age-/sex-matched healthy controls. Bioinformatics analysis was conducted to identify dysregulated proteins associated with stone formation. Results of proteomic analysis were verified by Western blotting in other three kidney stone patients and three healthy controls.

**Results:** Nine hundred and sixty proteins were identified with proteomic analysis, of which 831 were identified in the control group and 879 in the stone group. Sixteen proteins in urinary exosomes were found most significantly different between kidney stone patients and healthy controls. Gene ontology (GO) analysis showed that dysregulated proteins were enriched in innate immune response, defense response to bacterium and calcium-binding. S100A8, S100A9 and S100A12 were common in above three GO terms and were chosen for further study. Western blotting confirmed that the expression of these three S100 proteins was higher in urinary exosomes from kidney stone patients. In addition, S100 proteins were aggregated in urinary exosomes and it was difficult to detect them in urine.

**Conclusions:** Urinary exosomes from kidney stone patients are rich in S100 proteins and play a role in innate immune response, defense response to bacterium and calcium-binding.

**Keywords:** Urine; exosome; proteomic; S100 proteins; kidney stone

Submitted Jan 03, 2020. Accepted for publication Jun 15, 2020.

doi: 10.21037/tau-20-41

View this article at: <http://dx.doi.org/10.21037/tau-20-41>

## Introduction

Nephrolithiasis is one of the most common diseases in urology. Approximately 10% to 12% of the general population will suffer at least one kidney stone in their lifetime (1). The prevalence of kidney stones appears to be increasing in Western societies over the past four decades (2). Moreover, the recurrence rate for kidney

stones after the first treatment is reported to be as high as 50% in 10 years (3). Randall's plaque is an ectopic calcification in the interstitial tissue of the renal papilla. It consists of calcium phosphate and may serve as the nidus for a kidney stone (4). However, mechanism underlying the plaque formation remains uncertain. Transmission electron microscopy (TEM) shows that Randall's plaque

is surrounded by calcified membrane vesicles and collagen fibers, indicating that the plaque may nucleate via membrane vesicles and grows by addition of crystals at its periphery (5).

Exosomes are important vesicles for substance transport and information transmission between cells. Specific biomolecules (such as proteins, RNA, and DNA) can be encapsulated into exosomes and secreted into the extracellular milieu. Secreted exosomes could enter and regulate the physiological function of target cells, which leads to following pathophysiological changes (6). It has been reported that exosomes are involved in many diseases, such as immune reactions, tumor metastasis, neurodegeneration, and infection (7). Few studies have demonstrated the role of exosomes in stone formation. Jayachandran *et al.* report that the number of urinary CD63-positive (one of exosome markers) vesicles is greater in kidney stone patients than in healthy controls (8). In addition, oxalate could promote renal tubular epithelial cells to secrete exosomes (9). However, how these increased exosomes contribute to kidney stone is unclear. Singhto *et al.* reveal that exosomes from calcium oxalate-treated macrophages could enhance proinflammatory cytokine production and show greater binding capacity to crystals, which has been proved to be induced by proteins in exosomes (10).

Recently, urinary exosomes have attracted much attention because they can be collected noninvasively and exosomal proteins can act as biomarkers for certain disease-related pathophysiological events. Proteomic analysis of urinary exosomes has been conducted in several urinary diseases, such as bladder cancer, prostate cancer, and kidney diseases (11). While, there has been few studies evaluating the proteomics of urinary exosomes from kidney stone patients. In the present study, liquid chromatography-tandem mass spectrometry (LC-MS/MS) label-free quantitative proteomics was conducted to compare protein profiles in urinary exosomes between kidney stone patients and healthy controls. We aim to identify dysregulated proteins in urinary exosomes from kidney stone patients and to explore the potential role of exosomal proteins in nephrolithiasis.

## Methods

### *Participants and urine collection*

Patients who came to our department for surgical treatment

with kidney stones were invited to participate in the study. Those with urinary tract infection, hematuria or other organic diseases were excluded. Stone composition was analyzed postoperatively for every patient. People who came to our hospital for regular physical examination were invited to participate as healthy controls. Those with urinary stones, urinary tract infection, hematuria, or other systemic diseases were excluded. Each participant was asked to provide 200 to 300 mL first morning urine in a clean collection bag for exosome and protein extraction. The urine samples were stored at 4 °C and processed within 6 h. The study was conformed to the provisions of the Declaration of Helsinki (as revised in 2013). Ethical approval was obtained from the Institutional Review Board of Tongji Hospital, Tongji Medical College, Huazhong University of Science and Technology (2019S1147). Informed consent was obtained from the subjects.

### *Exosome isolation and purification*

Urine exosomes were isolated and purified using modified ultracentrifugation according to previous studies (12,13). Firstly, 150 mL urine was centrifuged at 2,000 g and 4 °C for 30 min to remove cells, debris, bacteria, and the majority of Tamm-Horsfall protein (THP). Next, the remaining macropolymers and THP were removed by further centrifugation at 17,000 g and 4 °C for 60 min. The supernatant was then concentrated to 25 mL by centrifugation in 100 kD ultrafiltration centrifuge tubes (Millipore, USA) at 3,000 g and 4 °C. The concentrated urine sample was then centrifuged at 200,000 g and 4 °C for 60 min. After that, the pellet was resuspended in 15 mL phosphate-buffered saline (PBS) and centrifuged again at 200,000 g and 4 °C for 60 min. Finally, the supernatant was discarded and the pellet (exosomes) was stored at -80 °C until use. The size distribution of exosomes was evaluated by nanoparticle tracking analysis (NTA) using ZetaView PMX 110 (Particle Metrix, Meerbusch, Germany). The morphology of exosomes was assessed by TEM using a Tecnai 12 G2 transmission electron microscope (FEI, Eindhoven, Netherlands).

### *Sample preparation for LC-MS/MS analysis*

Exosomes were resuspended in 100  $\mu$ L PBS and lysed in 200  $\mu$ L 1.5 $\times$  ice-cold lysis buffer [1% sodium deoxycholate (SDC), 100 mM Tris-HCl (Ph =8.5), 10 mM Tris

(2-chloroethyl) phosphate and 40 mM chloroacetamide] for 5 min. Afterward, the samples were boiled for 10 min and centrifuged at 12,000 g and 4 °C for 15 min to obtain the supernatant. Protein concentration was measured using the Bradford method (Beyotime Institute of Biotechnology, China). An equal amount of protein from each sample was used and diluted with double distilled H<sub>2</sub>O to reduce the SDC concentration to <0.5%. Trypsin was added at a ratio of 1:50 (enzyme: protein) and the mixture was digested overnight at 37 °C. The next day, an equal volume of 1% formic acid in ethyl acetate was added to stop the digestion. The digest was subjected to peptide purification using self-made styrene divinylbenzene-reversed phase sulfonate desalting columns. The peptide eluate was dried under vacuum and stored at -20 °C for later use.

### *LC-MS/MS analysis*

LC-MS/MS analysis was carried out in a hybrid quadrupole-time-of-flight (TOF) LC-MS/MS instrument (TripleTOF 5600, SCIEX) equipped with a nanospray source; 2 µg of peptides was dissolved in MS loading buffer (0.1% formic acid), loaded onto a C18 trap column (5 µm, 5 mm × 0.3 mm, Agilent Technologies) through an auto-sampler, and then eluted into a C18 analytical column (75 µm × 150 mm, 3 µm particle size, 100 Å pore size, Eksigent). Mobile phase A [3% dimethyl sulfoxide (DMSO), 97% H<sub>2</sub>O, 0.1% formic acid] and mobile phase B (3% DMSO, 97% acetonitrile, 0.1% formic acid) were used to establish a 100 min gradient, as follows: 0 min in 5% B, 65 min of 5–23% B, 20 min of 23–52% B, 1 min of 52–80% B, 80% B for 4 min, 0.1 min of 80–5% B, and a final step of 5% B for 9.9 min. The flow rate was constant at 300 nL/min. For information dependent acquisition mode analysis, each scan cycle consisted of one full-scan mass spectrum (with m/z ranging from 350 to 1,500, ion accumulation time 250 ms), followed by 40 MS/MS events (m/z ranging from 100 to 1,500, ion accumulation time 50 ms). The threshold for MS/MS acquisition activation was set to 120 cps for +2 to +5 precursors. Former target ion exclusion was set at 18 s.

### *Protein extraction*

Urine protein was extracted using acetone precipitation. Briefly, fresh urine was centrifuged at 1,500 rpm and 4 °C for 15 min. After that, the supernatant was mixed with ice-cold acetone at ratio of 1:1. The mixture was stored

overnight at -20 °C and then centrifuged at 12,000 g and 4 °C for 10 min. The pellet was dissolved in RIPA buffer (Beyotime Institute of Biotechnology, China) supplemented with phenylmethanesulfonyl fluoride (Beyotime Institute of Biotechnology, China). Briefly, the protein in purified exosomes was also extracted with RIPA buffer containing phenylmethanesulfonyl fluoride.

### *Western blot analysis*

The concentration of extracted protein was determined using the bicinchoninic acid protein assay kit (Beyotime Institute of Biotechnology, China). Equivalent amount of protein was separated using 10% or 15% sodium dodecyl sulfate-polyacrylamide gel electrophoresis. After being transferred to 0.2 µm polyvinylidene fluoride membranes, protein bands were blocked with 5% bovine serum albumin for 0.5 h and then incubated with primary antibody: rabbit anti-CD9 antibody (Abcam/ab92726, USA), mouse anti-Hsc70 antibody (Abcam/ab2788), rabbit anti-TSG101 antibody (Abcam/ab125011), rabbit anti-S100A8 antibody (Abcam/ab92331), rabbit anti-S100A9 antibody (Abcam/ab92507), or rabbit anti-S100A12 antibody (Abcam/ab37657) at 4 °C overnight. After that, membranes were incubated with secondary antibodies (Boster, China) conjugated with horseradish peroxidase for 1 h at room temperature and then visualized with a chemiluminescence imaging system (ChemiDoc™ MP Imaging System, Bio-Rad, USA).

### *Data analysis*

The raw data from the TripleTOF 5600 were analyzed with MaxQuant software (V1.6.2.10) using the Andromeda database search algorithm and the MaxLFQ function. Spectrum files were searched against the UniProt human protein database using the default parameters except for the followings: label-free quantification mode was used, the min ratio count was set to 1, and the “match between runs” function was checked. The search results were filtered using a 1% false discovery rate (FDR) (at both the protein and peptide levels) and were imported into the R version 3.6.1 environment for statistical analysis. Enrichment analysis of gene ontology (GO) terms including biological process, cellular component, and molecular function was performed via DAVID 6.8 (<https://david.ncifcrf.gov/>) and results were filtered using a hypergeometric test with FDR <0.05.

**Table 1** Demographic and clinical data of the studied subjects

ID	Age (y)	Gender	BMI (kg/m <sup>2</sup> )	Plasma Ca (mmol/L)	Plasma Pi (mmol/L)	Plasma Cr (μmol/L)	Number of stone	Stone size (mm <sup>2</sup> )	Stone side	Stone type
C1	34	Male	23.34	2.24	–	49	–	–	–	–
C2	37	Female	25.54	–	–	72	–	–	–	–
C3	27	Male	22.59	–	–	–	–	–	–	–
C4	30	Male	22.10	–	–	74	–	–	–	–
C5	26	Male	22.32	2.3	1.17	50	–	–	–	–
C6	30	Female	20.9	2.26	–	62	–	–	–	–
S1	31	Male	27.41	2.25	1.07	68	1	15×23	Left	Calcium oxalate monohydrate/carbonate apatite phosphate
S2	34	Male	24.14	2.17	1.29	76	1	32×20	Left	Calcium oxalate monohydrate
S3	32	Male	21.64	2.37	1.41	66	1	22×18	Right	Calcium oxalate monohydrate/magnesium ammonium phosphate stone
S4	27	Male	22.15	2.45	1	95	2	12×9/27×15	Left	Calcium oxalate monohydrate/calcium oxalate dihydrate
S5	29	Female	20.03	2.21	0.73	93	1	24×19	Right	Calcium oxalate monohydrate/carbonate apatite phosphate
S6	40	Female	21.65	2.24	1.14	73	1	17×20	Left	Calcium oxalate monohydrate/carbonate apatite phosphate

C, control group; S, stone group; BMI, body mass index.

## Results

### *Isolation and purification of urinary exosomes*

Twelve participants including six healthy controls and six kidney stone patients were involved in this study. Detailed information of participants was listed in *Table 1*. Primary components of all stones were calcium oxalate. Exosomes were isolated from morning urine via ultracentrifugation. TEM demonstrated that isolated samples consisted of vesicles with typical exosomal membrane morphology. NTA indicated that most vesicles showed a diameter of 60 to 90 nm and a distribution peak at 80 nm. Exosome markers (CD9, HSC70, and TSG101) were confirmed to be expressed highly in isolated vesicles by Western blotting. In addition, the expression of CD9, HSC70, and TSG101 in isolated vesicles was much higher than in the urine, which

further confirmed the successful isolation and purification of urinary exosomes (*Figure 1*).

### *Proteomic profiling of human urinary exosomes*

Urinary exosomal proteins from three healthy controls (C1, C2, and C3) and three kidney stone patients (S1, S2, and S3) were used for LC-MS/MS analysis. A total of 960 proteins were identified, of which 831 were identified in the control group and 879 in the stone group. Six hundred and ninety proteins were quantified at least twice in three replicates of each group and went to subsequent statistical analysis. When using absolute log<sub>2</sub> fold change (log<sub>2</sub>FC) >1 and P<0.05 as the screening criteria, 67 dysregulated proteins were identified between two groups (*Table 2*). In order to identify proteins with more significant

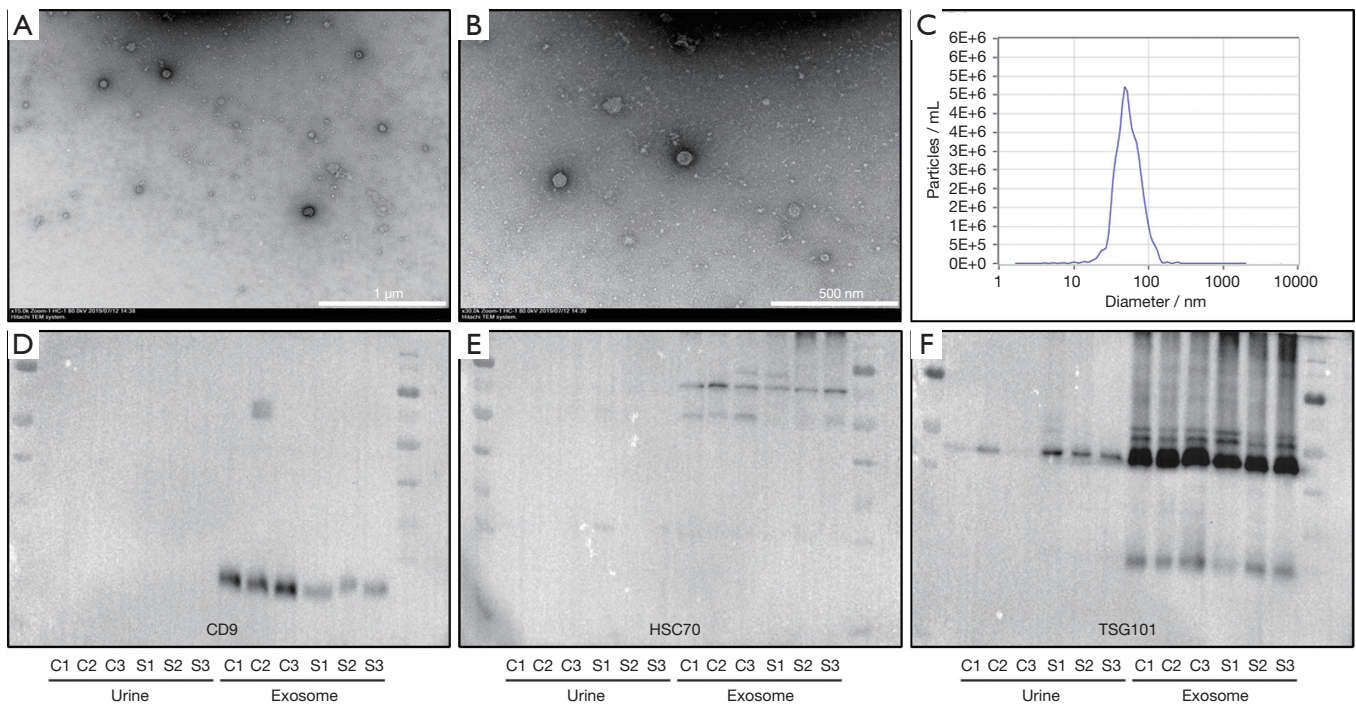


**Figure 1** Isolation and purification of urinary exosomes. (A,B) TEM demonstrates that isolated samples consisted of vesicles with typical membrane morphology. (C) NTA indicates that most vesicles had a size of 60–90 nm in diameter, with a peak at ~80 nm. (D,E,F) Western blotting confirmed that CD9, HSC70, and TSG101 are highly expressed in isolated exosomes but not in urine. TEM, transmission electron microscopy; NTA, nanoparticle tracking analysis.

difference, we fit  $\log_2FC$  values to a normal distribution and detected 5% thresholds for boundary as  $-3.403$  and  $3.164$  (Figure S1). Accordingly to the screening criteria ( $P < 0.05$ ,  $\log_2FC > 3.164$  or  $\log_2FC < -3.403$ ), we identified 16 most significantly dysregulated proteins. Among these dysregulated proteins, 14 were up-regulated and two were down-regulated in urinary exosomes from kidney stone patients (Figure 2).

#### Bioinformatics analysis of dysregulated proteins

To explore the possible biological functions of dysregulated proteins in urinary exosomes, we conducted GO analysis using the online DAVID database. Results demonstrated that the most enriched GO terms ( $FDR < 0.05$ ) are related to cellular component (blood microparticle, extracellular exosome, extracellular region, and extracellular space), biological process (innate immune response, defense response to bacterium, and retina homeostasis), and molecular function (immunoglobulin receptor binding

and RAGE receptor binding). Given that kidney stones are closely associated with calcium ions, we focused on another cluster named calcium ion binding ( $FDR > 0.05$  but  $P < 0.05$ ). S100A8, S100A9, and S100A12 proteins were found to be common in innate immune response, defense response to bacterium, and calcium ion binding. They were subsequently chosen for further study (Figure 3).

#### Western blotting confirmed that the expression of S100 proteins is higher in urinary exosomes from kidney stone patients

In order to validate the results obtained from LC-MS/MS analysis, western blotting was conducted to determine the level of urinary exosomal S100A8, S100A9, and S100A12 proteins in other three healthy controls (C4, C5, and C6) and three kidney stone patients (S4, S5, and S6). As shown in Figure 4, S100A8 and S100A9 were confirmed to be expressed higher in urinary exosomes from kidney stone patients than from healthy controls. Despite its low

**Table 2** List of dysregulated proteins in urinary exosomes between kidney stone patients and health controls

Abbreviation	Accession	Unique peptides	Sequence coverage (%)	Q-value	Score	Molecular function/biological process	Log <sub>2</sub> FC	P value
IGHM	P01871	15.00	46.10	0.00	323.31	Antigen binding/adaptive immune response	7.95	0.04
S100A8	P05109	15.00	91.40	0.00	323.31	Arachidonic acid binding/activation of cysteine-type endopeptidase activity involved in apoptotic process	6.57	0.03
S100A12	P80511	2.00	34.80	0.00	20.23	Calcium ion binding/antimicrobial humoral immune response mediated by antimicrobial peptide	6.40	0.02
PIGR	P01833	7.00	16.50	0.00	131.73	Polymeric immunoglobulin receptor activity/detection of chemical stimulus involved in sensory perception of bitter taste	4.92	<0.01
IGHG3	P01860	4.00	13.00	0.00	37.83	Antigen binding/B cell receptor signaling pathway	4.91	0.01
IGKC	P01834	5.00	68.20	0.00	84.23	Antigen binding/B cell receptor signaling pathway	4.91	0.02
A1AG1	P02763	2.00	12.40	0.00	16.10	Acute-phase response	4.87	0.03
S100A9	P06702	13.00	88.60	0.00	323.31	Calcium ion binding/activation of cysteine-type endopeptidase activity involved in apoptotic process	4.64	0.03
IC1	P05155	6.00	14.80	0.00	50.86	Serine-type endopeptidase inhibitor activity/aging	4.58	0.04
CERU	P00450	2.00	3.40	0.00	19.28	Chaperone binding/cellular iron ion homeostasis	3.65	0.01
APOA2	P02652	2.00	21.00	0.00	17.70	Apolipoprotein receptor binding/acute inflammatory response	3.56	0.03
CD44	P16070	2.00	2.80	0.00	13.37	Collagen binding/cartilage development	3.51	0.02
IGJ	P01591	3.00	11.90	0.00	18.30	Antigen binding/adaptive immune response	3.50	0.04
H4	P62805	6.00	52.40	0.00	151.20	DNA binding/cellular protein metabolic process	3.35	0.02
RET5	P82980	3.00	25.20	0.00	20.50	Retinal binding	-3.53	0.03
CRUM2	Q51J48	8.00	9.20	0.00	66.45	Aspartic-type endopeptidase inhibitor activity/cardiovascular system development	-4.66	<0.01
ANXA1	P04083	15.00	57.50	0.00	323.31	Cadherin binding involved in cell-cell adhesion/actin cytoskeleton reorganization	2.82	0.01
IGHA1	P01876	5.00	23.20	0.00	189.94	Antigen binding/antibacterial humoral response	2.78	0.02
LG3BP	Q08380	15.00	31.60	0.00	323.31	Scavenger receptor activity/cell adhesion	2.57	0.01
PIPNA	Q00169	1.00	4.40	0.00	11.71	Phosphatidylcholine binding/axonogenesis	2.17	0.03
TSN1	O60635	3.00	8.30	0.00	214.89	Cell migration	1.32	0.03
AKA12	Q02952	1.00	0.70	0.00	6.60	Adenylate cyclase binding/adenylate cyclase-inhibiting G protein-coupled receptor signaling pathway	1.12	0.03

**Table 2** (continued)

Table 2 (continued)

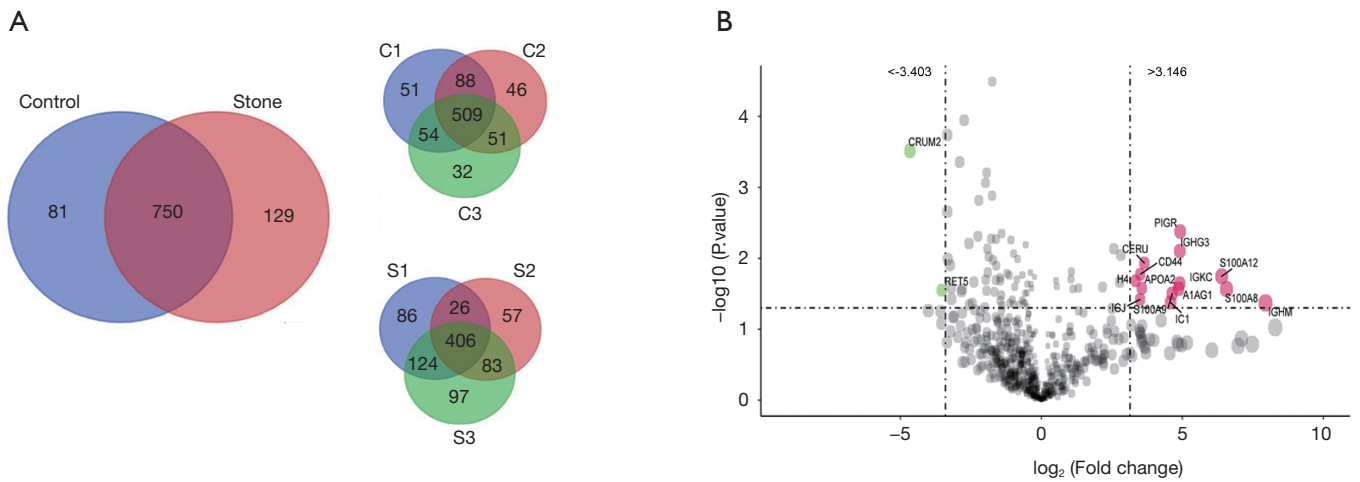
Abbreviation	Accession	Unique peptides	Sequence coverage (%)	Q-value	Score	Molecular function/biological process	Log <sub>2</sub> FC	P value
ANXA2	P07355	19.00	62.50	0.00	323.31	Bone sialoprotein binding/angiogenesis	1.06	0.02
CD63	P08962	2.00	5.00	0.00	216.86	Cell-matrix adhesion	1.05	0.02
KIF12	Q96FN5	14.00	24.50	0.00	230.36	ATPase activity/microtubule-based movement	-1.03	0.04
NHRF2	Q15599	4.00	16.90	0.00	30.76	Beta-catenin binding/protein-containing complex assembly	-1.08	0.01
LDHB	P07195	11.00	30.50	0.00	269.68	Identical protein binding/carbohydrate metabolic process	-1.12	0.04
S22A8	Q8TCC7	1.00	2.40	0.00	7.91	Inorganic anion exchanger activity/response to toxic substance	-1.14	0.02
CHM2A	O43633	8.00	24.30	0.00	187.99	Phosphatidylcholine binding/endosomal transport	-1.22	0.02
GSTA1	P08263	2.00	6.30	0.00	11.29	Glutathione peroxidase activity/epithelial cell differentiation	-1.39	0.05
GTR5	P22732	8.00	12.20	0.00	78.71	Fructose binding/carbohydrate metabolic process	-1.41	<0.01
VAT1	Q99536	3.00	9.20	0.00	32.12	Oxidoreductase activity/negative regulation of mitochondrial fusion	-1.42	0.03
ALDOB	P05062	12.00	36.30	0.00	323.31	ATPase binding/canonical glycolysis	-1.46	0.02
ITAV	P06756	3.00	3.50	0.00	17.85	Coreceptor activity/angiogenesis	-1.46	0.04
GDIA	P31150	1.00	2.90	0.00	6.94	GDP-dissociation inhibitor activity/negative regulation of axonogenesis	-1.46	0.02
F151A	Q8WW52	9.00	16.60	0.00	230.89	Single-pass membrane protein	-1.60	0.01
CMBL	Q96DG6	3.00	14.30	0.00	19.87	Hydrolase activity/xenobiotic metabolic process	-1.61	0.01
PTN23	Q9H3S7	2.00	1.20	0.00	18.04	Protein kinase binding/cellular response to cytokine stimulus	-1.61	0.02
ELOC	Q15369	1.00	8.90	0.00	6.75	Positive regulation of transcription elongation from RNA polymerase II promoter	-1.66	0.03
BHMT1	Q93088	13.00	44.80	0.00	205.59	Betaine-homocysteine S-methyltransferase activity/amino-acid betaine catabolic process	-1.72	0.01
VATG1	O75348	2.00	19.50	0.00	11.70	ATPase activity/cellular iron ion homeostasis	-1.74	<0.01
XPP2	O43895	23.00	42.00	0.00	323.31	Aminopeptidase activity	-1.75	<0.01
SC5A2	P31639	4.00	9.10	0.00	50.87	Glucose:sodium symporter activity/carbohydrate metabolic process	-1.78	0.01
SAM50	Q9Y512	1.00	2.60	0.00	11.94	Cellular protein-containing complex assembly	-1.86	0.01
SMIM1	B2RUZ4	1.00	15.40	0.00	6.80	Protein homodimerization activity	-1.90	0.02
CRUM3	Q9BUF7	1.00	14.20	0.00	12.83	Protein domain specific binding/bicellular tight junction assembly	-1.92	0.01
AQP1	P29972	5.00	25.30	0.00	171.08	Ammonium transmembrane transporter activity/ammonium transport	-1.94	<0.01

Table 2 (continued)

Table 2 (continued)

Abbreviation	Accession	Unique peptides	Sequence coverage (%)	Q-value	Score	Molecular function/biological process	Log <sub>2</sub> FC	P value
ACY3	Q96HD9	2.00	8.80	0.00	11.77	Aminoacylase activity/viral process	-1.94	0.03
DPEP1	P16444	19.00	51.30	0.00	323.31	Cysteine-type endopeptidase inhibitor activity involved in apoptotic process/antibiotic metabolic process	-1.97	0.02
DCXR	Q7Z4W1	3.00	16.40	0.00	31.85	Carbonyl reductase (NADPH) activity/D-xylose metabolic process	-1.98	<0.01
ACY1	Q03154	11.00	37.70	0.00	152.78	Aminoacylase activity/cellular amino acid metabolic process	-2.00	0.05
C2D1A	Q6P1N0	2.00	2.30	0.00	13.19	Cadherin binding/negative regulation of transcription by RNA polymerase II	-2.22	<0.01
ZDHC1	Q8WTX9	3.00	9.30	0.00	18.79	DNA binding/peptidyl-L-cysteine S-palmitoylation	-2.25	<0.01
LEG1	P09382	1.00	11.10	0.00	6.87	Carbohydrate binding/apoptotic process	-2.39	0.02
NDRG1	Q92597	1.00	6.30	0.00	11.85	Cadherin binding/cellular response to hypoxia	-2.45	0.04
STAM2	O75886	2.00	3.60	0.00	86.69	Endosomal transport	-2.55	0.05
EFNB1	P98172	2.00	8.40	0.00	13.49	Ephrin receptor binding/axon guidance	-2.57	0.01
BDH2	Q9BUT1	1.00	5.30	0.00	17.13	3-hydroxybutyrate dehydrogenase activity/epithelial cell differentiation	-2.74	<0.01
GGH	Q92820	4.00	19.20	0.00	46.61	Exopeptidase activity/neutrophil degranulation	-2.81	0.03
GSTA2	P09210	2.00	6.30	0.00	323.31	Glutathione transferase activity/epithelial cell differentiation	-2.83	0.03
CUTA	O60888	2.00	22.90	0.00	24.25	Copper ion binding/protein localization	-2.89	<0.01
B2MG	P61769	1.00	8.40	0.01	6.32	Identical protein binding/amyloid fibril formation	-3.18	0.04
GLYC	P34896	5.00	13.70	0.00	51.03	Amino acid binding/carnitine biosynthetic process	-3.19	0.03
GALM	Q96C23	2.00	10.50	0.00	27.70	Aldose 1-epimerase activity/galactose catabolic process via UDP-galactose	-3.25	0.01
TRFM	P08582	8.00	16.30	0.00	156.89	Iron ion binding/cellular protein metabolic process	-3.32	0.01
TBB5	P07437	1.00	6.10	0.00	12.56	GTPase activating protein binding/cell division	-3.34	<0.01
GNAI3	P08754	2.00	10.70	0.00	15.43	GDP binding/adenylate cyclase-inhibiting G protein-coupled receptor signaling pathway	-3.34	<0.01

FC, fold change.



**Figure 2** Proteomic profiling of human urinary exosomes. (A) A total of 960 urinary exosomal proteins were identified, of which 831 were identified in the control group and 879 in the stone group. (B) With screening criteria of  $P < 0.05$  and  $\log_2\text{FC} > 3.164$  or  $\log_2\text{FC} < -3.403$ , 16 proteins were found to be most significantly different between two groups.

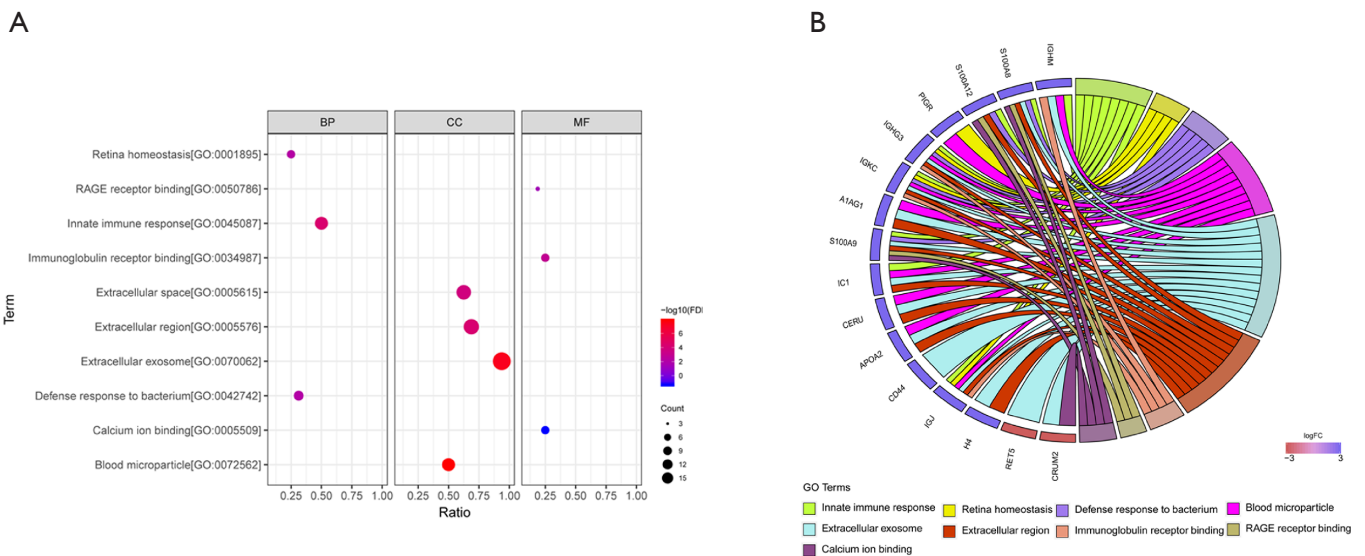


**Figure 3** Gene ontology analysis of dysregulated proteins. (A) Dysregulated proteins were mainly enriched in cellular component (blood microparticle, extracellular exosome, extracellular region, and extracellular space), biological process (innate immune response, defense response to bacterium, and retina homeostasis), and molecular function (immunoglobulin receptor binding and RAGE receptor binding). (B) S100A8, S100A9, and S100A12 were common in innate immune response, defense response to bacterium, and calcium ion binding.

abundance in urinary exosomes, the expression of S100A12 was also higher in urinary exosomes from kidney stone patients. Detection of these three S100 proteins in urine was difficult, indicating their specific aggregation in urinary exosomes.

### Discussion

Kidney stone formation involves not only urinary crystal supersaturation but also the interaction between crystals, proteins, membrane vesicles, collagen fibers,

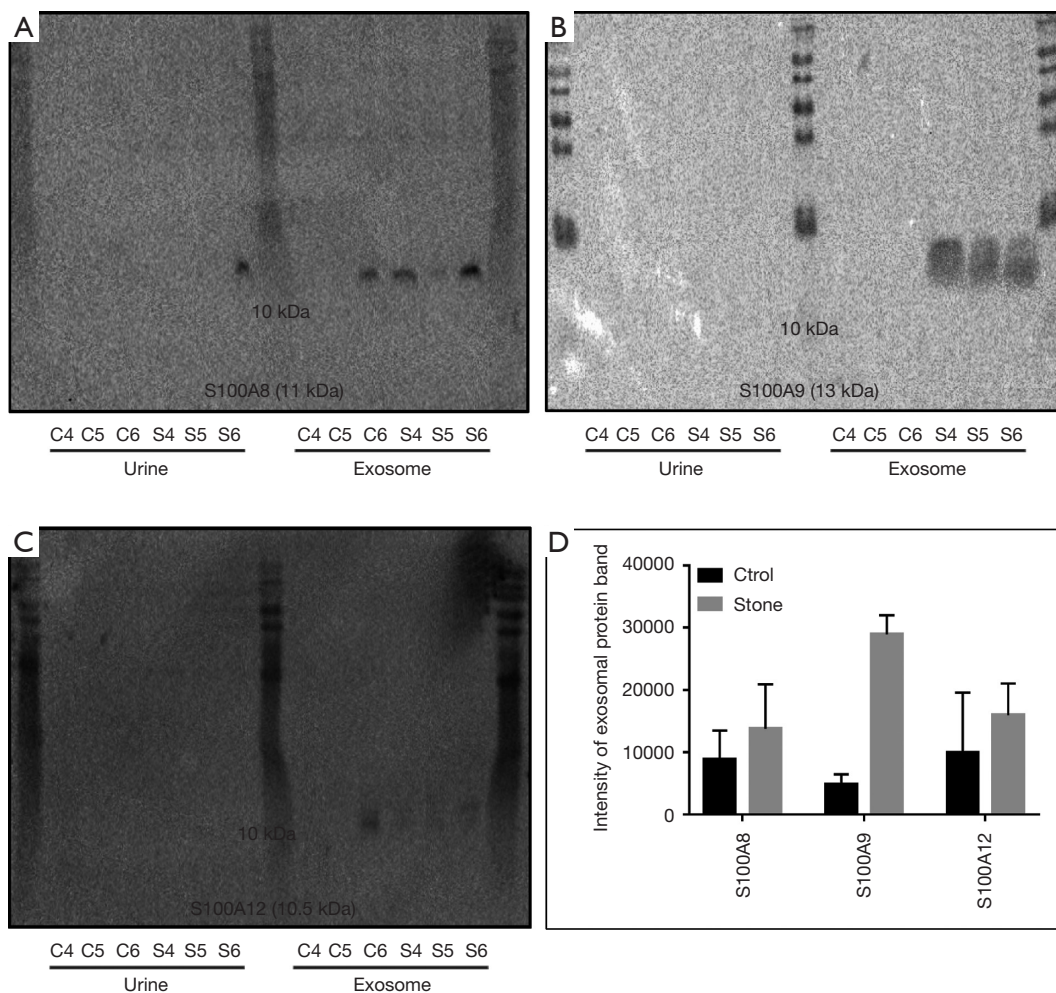


**Figure 4** Verification of proteomic results in other six participants. (A,B) The expression of S100A8 and S100A9 is higher in urinary exosomes from kidney stone patients. (C) The abundance of S100A12 was low in urinary exosomes, but its expression was also higher in exosomes from kidney stone patients than in those from healthy controls. It was difficult to detect these three S100 proteins in urine. (D) Intensity of protein bands from exosomes.

and cells. Electron microscopic examination of the renal papillary tissue at stone attachment sites has detected many membrane vesicles containing nucleated calcium phosphate crystals (14). Increased urinary exosomal vesicles are reported to be associated with kidney stones. Shyong *et al.* also demonstrate that calcium phosphate particles stimulate the secretion of exosomes from cultured cells (15). The pathophysiological function of exosomes is mainly dependent on the substances they contain, including proteins, RNA and DNA. Urinary exosomes contain cell-specific proteins from every segment of the nephron, which is a potential source of valuable urinary biomarkers for diseases of the kidney and urinary tract (16).

We hypothesize that not only concentration, but also the protein profiles are different between urinary exosomes from kidney stone patients and healthy people. To the best of our knowledge, the present study represents the first attempt to use proteomic technology to compare urinary exosomal protein profiles between kidney stone patients and healthy controls.

Despite the fact that we included participants without urinary tract infection and hematuria, the function of dysregulated proteins in urinary exosomes from kidney stone patients focused on immune responses and defense responses to bacteria. Similarly, previous studies have also demonstrated that inflammatory processes play an

important role in kidney stone formation and protein components of inflammation contribute to the abundant stone matrix proteome (17). Interestingly, we also found that some dysregulated inflammatory proteins played a role in calcium binding, namely calgranulin proteins (S100A8, S100A9, and S100A12). They were confirmed to be enriched in the urinary exosomes but not urine, suggesting that urinary exosomal S100 proteins may provide potential biomarkers for nephrolithiasis.

S100A8, S100A9, and S100A12 are members of the S100 calcium-binding protein family, which is characterized as a helix-loop-helix motif, charged amino acid residues and high affinity for calcium ion. Their expression is abundant in neutrophils and inducible in macrophages. The S100 calcium-binding protein family plays a prominent role in regulating inflammation and immune responses, including recruitment of leukocytes, production of cytokines and promotion of leukocyte adhesion and migration (18). In addition, studies have demonstrated that S100 proteins play a role in the calcification of atherosclerotic plaques. New *et al.* found that matrix vesicles released from calcium phosphate stimulated macrophages are rich in S100A9 and show high calcification and aggregation potential (19). Chellan *et al.* report that S100A12 transgenic mice could develop vascular calcification spontaneously. Overexpression of S100A12 promotes osteoblast-like cell transformation and calcification in vascular smooth muscle cells (20). Similarities between vascular calcification plaque and Randall's plaque have been reported and osteoblast-like cell transformation of renal tubular epithelial cells is also observed during stone formation (21).

Renal tubular and collecting duct epithelium cells have also been reported to express S100 proteins (22). Unlike some classic proteins involved in nephrolithiasis [such as osteopontin (OPN) and CD44], the role of S100 proteins in stone formation is rarely studied in basic research. Instead, almost all studies focusing on protein profiles of kidney stones report that S100 proteins exist in the stone matrix (23-26). These calgranulin proteins are not only abundant in calcium oxalate stones, but also in uric acid, magnesium ammonium phosphate and matrix stones. In addition, S100A8 and S100A9 have even been detected in demineralized hydroxyapatite, brushite, uric acid, calcium oxalate monohydrate, and calcium oxalate dihydrate urinary crystals precipitated from healthy human urine samples (27). More importantly, S100 proteins are restricted to the inner core but not the outer matrix of kidney stones (28), indicating that they contribute to the initial nucleation of crystals.

Boonla *et al.* also report that S100A8 is overproduced by infiltrated leukocytes in the kidneys from nephrolithiasis patients (29). These findings highlight the relevance of S100 proteins in inflammatory pathogenesis of urolithiasis and indicate that S100 proteins are involved in the nucleation of kidney stone.

There are several limitations in our study. Firstly, the number of participants is small and studies with more participants in the future are needed to validate the current findings. Secondly, the average age of participants seems young and primary component of stones from every patient was calcium oxalate, which show a selection bias and limit the applicability to calcium oxalate stones. Thirdly, this is a descriptive proteomic study. More basic research is needed to evaluate the role of exosomal S100 proteins in stone formation.

## Conclusions

Urinary exosomes from kidney stone patients are rich in S100 proteins and mainly play a role in innate immune response, defense response to bacterium and calcium-binding.

## Acknowledgments

*Funding:* This work was supported by the National Natural Science Foundation of China (grant number 81974092 and 81570631).

## Footnote

*Data Sharing Statement:* Available at <http://dx.doi.org/10.21037/tau-20-41>

*Conflict of Interest:* All authors have completed the ICMJE uniform disclosure form (available at <http://dx.doi.org/10.21037/tau-20-41>). The authors have no conflicts of interest to declare.

*Ethical Statement:* The authors are accountable for all aspects of the work in ensuring that questions related to the accuracy or integrity of any part of the work are appropriately investigated and resolved. The study was conformed to the provisions of the Declaration of Helsinki (as revised in 2013). Ethical approval was obtained from the Institutional Review Board of Tongji Hospital, Tongji Medical College, Huazhong University of Science and

Technology (2019S1147). Informed consent was obtained from the subjects.

*Open Access Statement:* This is an Open Access article distributed in accordance with the Creative Commons Attribution-NonCommercial-NoDerivs 4.0 International License (CC BY-NC-ND 4.0), which permits the non-commercial replication and distribution of the article with the strict proviso that no changes or edits are made and the original work is properly cited (including links to both the formal publication through the relevant DOI and the license). See: <https://creativecommons.org/licenses/by-nc-nd/4.0/>.

## References

1. Coe FL, Evan A, Worcester E. Kidney stone disease. *J Clin Invest* 2005;115:2598-608.
2. Scales CD Jr, Smith AC, Hanley JM, et al. Prevalence of kidney stones in the United States. *Eur Urol* 2012;62:160-5.
3. Uribarri J, Oh MS, Carroll HJ. The first kidney stone. *Ann Intern Med* 1989;111:1006-9.
4. Daudon M, Bazin D, Letavernier E. Randall's plaque as the origin of calcium oxalate kidney stones. *Urolithiasis* 2015;43:5-11.
5. Khan SR, Rodriguez DE, Gower LB, et al. Association of Randall plaque with collagen fibers and membrane vesicles. *J Urol* 2012;187:1094-100.
6. Théry C, Zitvogel L, Amigorena S. Exosomes: composition, biogenesis and function. *Nat Rev Immunol* 2002;2:569-79.
7. Kourembanas S. Exosomes: vehicles of intercellular signaling, biomarkers, and vectors of cell therapy. *Annu Rev Physiol* 2015;77:13-27.
8. Jayachandran M, Lugo G, Heiling H, et al. Extracellular vesicles in urine of women with but not without kidney stones manifest patterns similar to men: a case control study. *Biol Sex Differ* 2015;6:2.
9. He Z, Guan X, Liu Y, et al. Alteration of exosomes secreted from renal tubular epithelial cells exposed to high-concentration oxalate. *Oncotarget* 2017;8:92635-42.
10. Singhto N, Kanlaya R, Nilnumkhum A, et al. Roles of macrophage exosomes in immune response to calcium oxalate monohydrate crystals. *Front Immunol* 2018;9:316.
11. Moon PG, You S, Lee JE, et al. Urinary exosomes and proteomics. *Mass Spectrom Rev* 2011;30:1185-202.
12. Gonzales PA, Pisitkun T, Hoffert JD, et al. Large-scale proteomics and phosphoproteomics of urinary exosomes. *J Am Soc Nephrol* 2009;20:363-79.
13. He L, Zhu D, Wang J, et al. A highly efficient method for isolating urinary exosomes. *Int J Mol Med* 2019;43:83-90.
14. Khan SR, Canales BK. Unified theory on the pathogenesis of Randall's plaques and plugs. *Urolithiasis* 2015;43:109-23.
15. Shyong YJ, Chang KC, Lin FH. Calcium phosphate particles stimulate exosome secretion from phagocytes for the enhancement of drug delivery. *Colloids Surf B Biointerfaces* 2018;171:391-7.
16. Merchant ML, Rood IM, Deegens JKJ, et al. Isolation and characterization of urinary extracellular vesicles: implications for biomarker discovery. *Nat Rev Nephrol* 2017;13:731-49.
17. Sun AY, Hinck B, Cohen BR, et al. Inflammatory cytokines in the papillary tips and urine of nephrolithiasis patients. *J Endourol* 2018;32:236-44.
18. Bresnick AR, Weber DJ, Zimmer DB. S100 proteins in cancer. *Nat Rev Cancer* 2015;15:96-109.
19. New SE, Goetsch C, Aikawa M, et al. Macrophage-derived matrix vesicles: an alternative novel mechanism for micro calcification in atherosclerotic plaques. *Circ Res* 2013;113:72-7.
20. Chellan B, Sutton NR, Hofmann Bowman MA. S100/RAGE-mediated inflammation and modified cholesterol lipoproteins as mediators of osteoblastic differentiation of vascular smooth muscle cells. *Front Cardiovasc Med* 2018;5:163.
21. Joshi S, Clapp WL, Wang W, et al. Osteogenic changes in kidneys of hyperoxaluric rats. *Biochim Biophys Acta* 2015;1852:2000-12.
22. Pillay SN, Asplin JR, Coe FL. Evidence that calgranulin is produced by kidney cells and is an inhibitor of calcium oxalate crystallization. *Am J Physiol* 1998;275:F255-61.
23. Okumura N, Tsujihata M, Momohara C, et al. Diversity in protein profiles of individual calcium oxalate kidney stones. *PLoS One* 2013;8:e68624.
24. Wesson JA, Kolbach-Mandel AM, Hoffmann BR, et al. Selective protein enrichment in calcium oxalate stone matrix: a window to pathogenesis? *Urolithiasis* 2019;47:521-32.
25. Canales BK, Anderson L, Higgins L, et al. Proteome of human calcium kidney stones. *Urology* 2010;76:1017.e13-20.
26. Martelli C, Marzano V, Iavarone F, et al. Characterization of the protein components of matrix stones sheds light

- on S100-A8 and S100-A9 relevance in the inflammatory pathogenesis of these rare renal calculi. *J Urol* 2016;196:911-8.
27. Thurgood LA, Ryall RL. Proteomic analysis of proteins selectively associated with hydroxyapatite, brushite, and uric acid crystals precipitated from human urine. *J Proteome Res* 2010;9:5402-12.
28. Mushtaq S, Siddiqui AA, Naqvi ZA, et al. Identification of myeloperoxidase, alpha-defensin and calgranulin in calcium oxalate renal stones. *Clin Chim Acta* 2007;384:41-7.
29. Boonla C, Tosukhowong P, Spittau B, et al. Inflammatory and fibrotic proteins proteomically identified as key protein constituents in urine and stone matrix of patients with kidney calculi. *Clin Chim Acta* 2014;429:81-9.

**Cite this article as:** Wang Q, Sun Y, Yang Y, Li C, Zhang J, Wang S. Quantitative proteomic analysis of urinary exosomes in kidney stone patients. *Transl Androl Urol* 2020;9(4):1572-1584. doi: 10.21037/tau-20-41

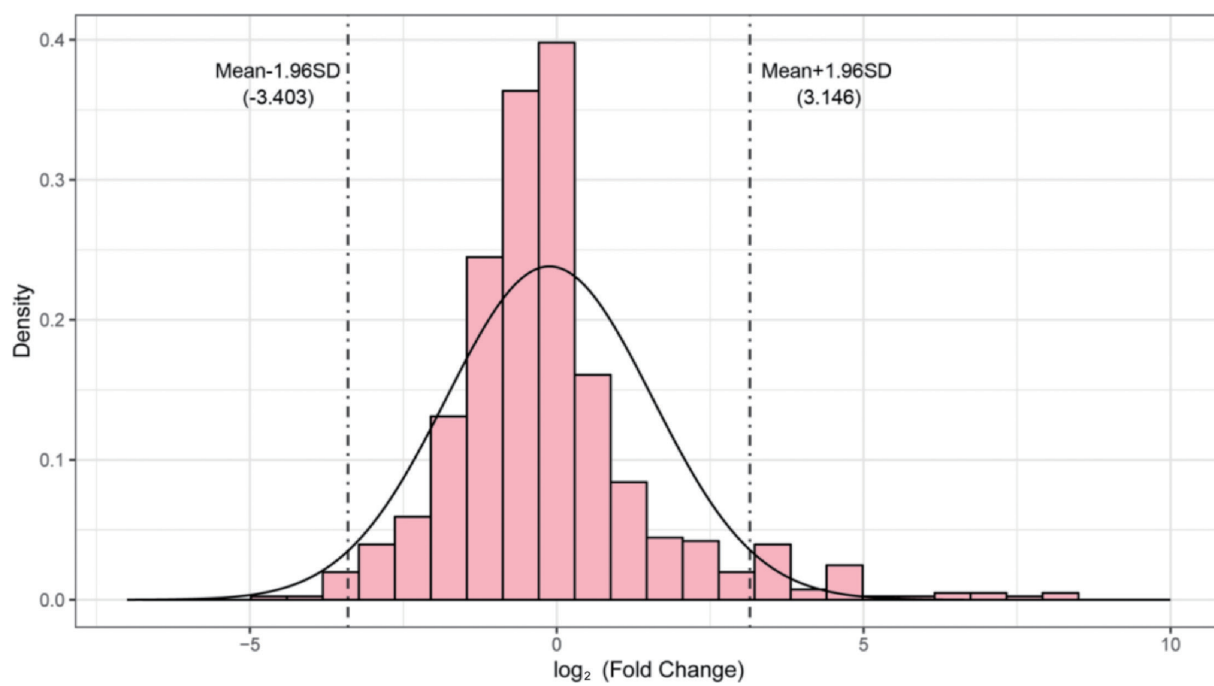


**Figure S1** We fit the normal distribution with  $\log_2\text{FC}$  and the 5% threshold for  $\log_2\text{FC}$ , boundary is  $-3.403$  and  $3.164$  respectively.